Non-rigid registration method to assess the reproducibility of breath-holding with ABC in lung cancer

D. Sarrut[PhD,1,2], V. Boldea[2] M. Ayadi[1], JN. Badel[1], C. Ginestet[1] S. Clippe[1]

Address 1 : Department of Radiotherapy, Centre Léon Bérard, Lyon, France
Address 2 : LIRIS laboratory, Université Lumière Lyon 2, Lyon, France

Corresponding author : David Sarrut, Department of Radiotherapy, Centre Léon Bérard, 28 rue Laennec, 69008 Lyon, France, Phone number : 33 4 78 78 51 51, Fax number : 33 4 78 78 26 26, dsarrut@univ-lyon2.fr

Abstract—

Purpose: **To study the interfraction reproducibility of breath-holding using Active Breathing Control (ABC). To develop computerized tools to evaluate 3D intra-thoracic motion in each patient.**

Methods and materials: **Since June 2002, 11 patients with non-small-cell lung cancer (NSCLC) enrolled in a phase II trial have undergone four CT scans: one acquired during free-breathing (reference) and three using the ABC device. Patient breath was held at the same predefined phase of the breathing cycle (about 70% of the vital capacity) using ABC device, then patients received 3D-conformal radiotherapy. Automated computerized tools were developed to analyze lung interfraction deformation with 3D non-rigid registration.**

Results: **All patients but one were safely treated with ABC for 7 weeks. For 6 patients, lung volume differences were below 5% and mean (standard deviation) intra-pulmonary 3D displacements were between 2.3(1.4) and $4\,mm(3.3)$, slightly greater in the inferior part of the lung than above. For 2 patients, we detected volume changes greater than $300\,cc$ and displacements greater than $10\,mm$, due to atelectasia and emphysema.**

Conclusion: **Breath holding with ABC was effective in 6 patients, whereas discrepancies were clinically accountable in 2. The proposed 3D non-rigid registration method allows personalized evaluation of breath-holding reproducibility with ABC. It will be used to adapt patient-specific internal margins.**

Keywords— **breath-holding, non-rigid registration, lung cancer**

I. INTRODUCTION

Organ motion during the respiratory cycle is known to be a source of inaccuracy in treatment delivery because it leads to tumor displacement and suboptimal dose delivery. Imaging studies using fluoroscopy have shown that tumors and organs can move from $10\,mm$ to more than $30\,mm$ (for diaphragm) during the breathing cycle [1], [2]. A main challenge for non-small-cell lung cancer (NSCLC) radiotherapy is the ability to spare surrounding normal tissues while providing prescribed doses to the tumor, because *1)* dose escalation seems to yield superior outcomes [3], [4], [5] and *2)* normal lung tissue is very sensitive to radiation: Tsujino et al. [6], [7] have correlated the risk of developing severe pneumonitis to the volume of irradiated lung.

Incorporating organ motion can be achieved with several approaches. The most common approach consists in adapting internal margins (as defined in ICRU Report 62) [8], [9], [10], [11]. The major drawback of this techniques is that it is based on averaged, predictable, regular, reproducible organ and tumor motion models, while numerous studies have shown that lung tumor motion is more complex than a simple cyclic process [5], [12], [13], [14], [15], [16], [17].

Another promising approach is synchronizing radiation delivery with patient breathing: the treatment beam is enabled at predetermined intervals during the breathing cycle while the patient breathes freely [18], [19], [11], [17], [12]. However, this gating technique would require invasive placement of internal fiducial markers, or depend on a correlation between external and internal movements, which has not yet been well established [12].

We are interested here in an intermediate approach consisting in immobilizing the organs by breath-holding. Intrafraction motions are motion that occur during the delivery of radiation treatment, during a patient breath-hold (BH). Interfraction motions are changes or displacements of the tumor from one day to the next. Movements measured during the BH phase are considered negligible ($1\,mm$) with active BH [20], [21], [22], and estimated between 1.0 and $1.8\,mm$ with self BH [18], [8], [23]. The interfraction reproducibility varies with the phase of the respiratory cycle: it tends to be better at the end of normal expiration/inspiration BH phases than at deep inspiration BH for some authors [24], [20] tough contrary findings have also been reported [25]. However, deep inspiration BH also increase the lung volume and consequently decrease the mass of irradiated lung.

The goal of this study was to develop a non-rigid 3D registration method to systematically evaluate the interfraction reproducibility of BH with Active Breath Control (ABC) device. This approach allows to estimate the 3D displacement of each point between different CT scans and thus helps determine adapted internal margins.

II. METHODS AND MATERIALS

A. Data acquisition

A.1 Patients

Since June 2002, 11 patients with non-small-cell lung cancer (NSCLC) have been enrolled in a phase II trial. Radical radiotherapy was indicated because of potentially resectable but inoperable T1-T4, N0-N1, M0 NSCLC. All patients had severe respiratory insufficiency. In all cases, informed consent was obtained in accordance with French laws and with the procedures of the local Consultative Committee for the Protection of Participants in Biomedical Rsearch (CCPPRB).

A.2 Active Breathing Control device

The ABC (Active Breathing Control) device proposed by Wong et al. [1] allows for temporary immobilization of respiratory motion by implementing a BH at a predefined lung volume (relatively to the end of normal expiration, corresponding to the functional residual capacity) and air flow direction. When the patient reaches this predefined lung volume level during either inspiration or expiration, his airflow is temporarily blocked, thereby immobilizing breathing motion. The radiation source will be turned on and off during this period. To our knowledge, several studies have reported the use of ABC for liver [20], breast [22], [26], [27], [28], [29], [30] and lung cancers [1], [31], [21], [4].

A.3 Patient breath-holding with ABC

We used 2 ABC devices from Elekta (called *Active Breathing Coordinator*), one in the treatment room, the other one in the CT scan room. The two devices were calibrated with a 3L syringe. Patient breath was held at the same given phase of the breathing cycle, mDIBH (medium DIBH),corresponding to about 70%/75% of the vital capacity depending on the patient. All patients followed an initial training session to determine the maximum time gate they could reach relatively comfortably. This is particularly important because they had to repeat this step as many times as the total number of fractions required. The training session and preparation of patient immobilization took approximately 90 minutes. Verbal instructions were given all along the sessions. BH duration was between 15-20 sec, tough additional time could sometimes be allocated, depending on patient ability. First sessions were generally longer than the following, according to the patient's habituation. Patient immobilization was achieved using an alpha-cradle [22].

A.4 CT scans

Each patient had one CT scan acquired during free-breathing (FB, reference) and three acquired in BH mode using the ABC device. All CT scans were acquired on a Picker© PQ 2000. FB were acquired in axial mode and BH in spiral mode (spiral pitch of 1.5). FB scans were acquired in time with an average respiratory cycle, about 4 sec [5] in order to reduce artifact. BH scans were acquired over several BH sessions (7 or 8 BH depending on patient ability), as described in [4]. Slices (5mm thickness) were then stacked into a 3D volume. Consistency between consecutive slices was checked by visual inspection. The total acquisition session took about 90 minutes for the 4 CT scans. The time interval between the three BH acquisitions ranged from 2 hours to several days (patient leaving the room after each session), allowing interfraction comparisons. Final 3D dataset size range was 512×512 with $[60 - 70]$ slices. Eight datasets (out of 11) were available, with 24 CT scans acquired with ABC and 8 without.

A.5 Treatment

Patients then received 3D-conformal radiotherapy. The treatment consisted in two steps : one step using 6 coplanar static fields with MLC for dose up to 40-50Gy and the second one using 6 boost fields and MLC to a final dose of 70 Gy (using Elekta© SL20 accelerator). Each field was delivered while the patient BH maintained with ABC device at the pre-determined threshold, fitted to the lung DVH.

B. Lung volume comparison

Our first goal was to develop a reproducible tool for automatic quantification of lung volumes (left/right/whole lung). The first step consisted in segmenting the whole lung with simple thresholding, as described in [1], [31], [21]. Voxels with density below a given threshold were selected. These voxels correspond to the air (outside and inside the patient), the lung and the gas (in the patient bowel for example). Then, the resulting binary image was labeled with a automated 3D connected components labeling algorithm (voxel neighborhood with 26-adjacency). Finally, only one connected component corresponding to the whole lung was automatically selected (selection corresponding to the second largest component, the first one being the air outside the patient).

This technique does not require any user intervention, except setting the threshold. The measured lung volume is highly dependent on the chosen threshold (for example, it defines what part of the airways should be included in the lung volume). The choice of an "optimal" threshold was not very relevant to our problematic because we wanted to *compare* volumes over the three CT taken from the same patient. Moreover, it is not clear whether such an "optimal" value really exists. Hence, rather than using a single fixed threshold we chose to compare several lung volume measurements obtained from a range of 10 threshold values (between -200 and -600 HU), centered near an automatic threshold, computed by the technique described in [32]. This produced a total of $8(patients) \times 3(CT) \times 10(threshold) = 240$ segmentations. In the following LVD denotes the lung volume difference between 2 CT scans of a given patient.

B.1 Segmentation variability analysis

Our first study evaluated the influence of threshold variations on the LVD. We first investigated the relation between threshold and lung volume among the three CT of

each patient. The threshold range was chosen such that the relation was quasi linear. The slope of this linear relation and extrema values of lung volumes were computed and compared.

B.2 Lung volume difference analysis

For each patient, the LVD between each pair of CT scans were computed for each threshold level. Differences are expressed in *cc* and in percentage of the initial lung volume. When the LVD was greater than 7%, we investigated the distribution of this difference between the left and right lungs. Lung segmentation was performed with morphological mathematics tools. First, previously computed lung volume was progressively eroded (by a fixed number of erosion steps of 1-voxel kernel radius) in order to break the junction between the two lungs. Then, 3D connected components labeling was performed, and the two largest remaining components were labeled as right and left lungs. Finally, the two components were dilated to the initial whole lung volume in order to propagate the left and right labels. The trachea was also segmented using a similar technique. Mean lung density was computed on each CT scan.

Our objective was not to perform a perfect segmentation but to develop an automated reproducible technique permitting to compare volumes using the same basis. Figure 1 shows an example of the segmentation result.

C. Motion estimation with non-rigid registration algorithm

The 3D displacement of each individual lung point between two acquisitions was estimated using image registration methods. Registering two images is finding a geometrical transformation that will pair as best as possible each point in one image (called reference image, denoted by I) with its correspondent in the second image (called object image, denoted by J) [33]. There are two main classes of transformations (denoted by T): rigid (translations, rotations) and non-rigid (allowing local deformations). The complexity of lung motion can not be reduced to a simple rigid transformation, so we used a 3D non-rigid registration method to estimate local deformations between CT acquisitions.

Non-rigid methods can be classified into 2 categories: sparse vector field methods and dense vector field methods. A sparse vector field method requires a set of control points (or landmarks) in the reference image with known correspondences in the object image. The final transformation is computed by using a deformation model (such as thin-plate spline [34]) to interpolate the point displacements. However, defining or detecting point correspondences between two different acquisitions is difficult in lung, and the final result highly depends on the accuracy of the corresponding points. Dense vector field methods compute a displacement vector for each point of the volume, leading to potentially more robust point correspondence ; no control points are needed.

We used a home-made method based on the algorithm proposed by Thirion and Cachier [35], [36], [37]. The method, see [38], is a modified version of the optical flow technique [39] allowing to retrieve large and small displacements. This iterative intensity-based method, compares image intensities (grey-levels) and requires no segmentation. Each iteration has two steps: pairing and regularization. *(1)* The corresponding point of $\boldsymbol{x}$ at iteration i, denoted by $u_i(\boldsymbol{x})$, is estimated according to the local gradient of the reference image (eq 1, $J \circ T$ denotes the composition, ∇ denotes the gradient operator, α is a parameter allowing to control the maximum local displacement in one iteration). This approach relies on the assumption of a grey level intensity conservation between two acquisitions (both images are acquired with the same protocol). *(2)* The regularization step consists in avoiding spatial incoherences (for example two neighboring points with opposite motions). We used a 3D Gaussian recursive filter [40], that was shown to be similar (under some assumptions) to the viscous fluid regularisation method [41].

$$u_i(\boldsymbol{x}) = \frac{I(\boldsymbol{x}) - J \circ T_{i-1}(\boldsymbol{x})}{\| \nabla I \|^2 + \alpha^2 (I(\boldsymbol{x}) - J \circ T_{i-1}(\boldsymbol{x}))^2} \nabla I \qquad (1)$$

This method results in a dense 3D deformation field, computed every $2\,mm$ in the in-plane dimension, between two CT scans: at each voxel of the first CT scan, a 3D vector points to the corresponding voxel in the second CT scan.

C.1 Residual error

The resulting deformation field is composed of two parts: a global rigid deformation (corresponding to the misalignment of the patient between the two acquisitions) and a deformation that we called the residual error (corresponding to lung motion differences between two BH). To find this residual error, we applied a 3D rigid registration algorithm [42], [43] that we adapted to favor the registration of the rigid bony structures. Accuracy was verified by visual checking. The residual error was then obtained by subtracting this rigid transformation from the deformation field obtained by non-rigid registration.

C.2 Data computation

Each CT acquisition was alternatively used as object or reference image. For each patient, we computed 6 rigid and 6 non-rigid registrations, leading to a total of 48 rigid and 48 non-rigid registrations. Each vector fields represents $256 \times 256 \times 70 = 4.6$ million vectors, amounting to $52.5Mb$ in total (each vector is defined by 4 bytes per coordinate). There are from $870,000$ to 2 million vectors for each lung depending on the patient. We also divided the lung volume into 6 regions (from inferior-to-superior regions, inferior 10%, intermediate 20% $\times$ 4, and superior 10%) as described in [22]. We analyzed the displacement by computing mean norm displacements inside the lung and on the lung surface only. For comparison purpose with [22], we developed an algorithm to compute distance to agreement (DTA). The DTA between two lung surfaces averages the distance of each point of the first lung surface to the

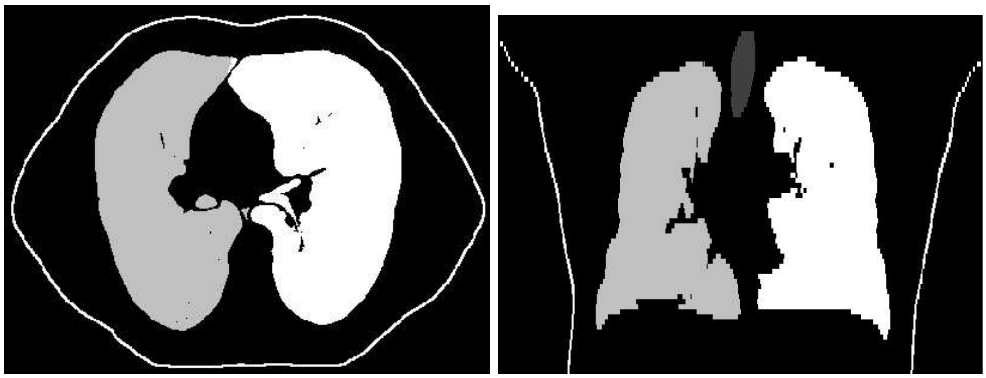

Fig. 1
Slices (axial and coronal) of segmented CT. Trachea, left and right lungs are displayed using different gray levels. Patient boundaries are displayed in white.

closest point in the second surface. Our method used a distance map algorithm [44] to compute the distance of each voxel in a volume to the closest point on the lung surface. Final DTA computation was performed by summing the distances obtained for points belonging to the surface. The computation time for the whole process (segmentation, vector fields, measurements) with a $512 \times 512 \times 70$ image took less than 30 minutes using a standard PC (2.7 Gz, 1Go RAM, Linux).

C.3 Visualization

Dense 3D vector fields are difficult to visualize because of the amount of information provided. We generated three kinds of images for better visualization and interpretation of the residual error. Figure 2 presents projected 3D vector fields on two slices. Arrows correspond to the residual error between two BH, showing the displacement of the surrounding points. Density windowing of the slices was adapted for visual purpose in order to observe both low (inside lung) and high density points (rigid structures). The 2D projection of the vector field fails to convey the third dimension of the information: the normal displacement of the projected vector. The axial slice is shown again in figure 3 on which two colors depict the cranio-caudal displacement. Green corresponds to displacements towards patient's head and blue towards patient's foot. Green and blue intensities are scaled as a function of the norm of the displacement Figure 4 illustrates the norm of the displacement vectors (dark red corresponding to small, and light red to large displacements).

III. RESULTS

A. Lung volume

A.1 Segmentation variability analysis

Lung volume is quasi-linear according to the threshold (mean of asymptotic standard errors lower than 0.3%). The relationship between threshold and volume was found to remains quasi-constant among the 3 CT scans of each patient (differences between extrema volumes were lower than $60cc$ or 4%), but they differed from one patient to another (the slope of the linear relationship between threshold and volume ranged from 1.1 to 2.0).

Volume variations according to the different thresholds were very consistent: for each patient, the standard deviation (over the 10 segmentations) between LVD (expressed in percentage of the initial volume) varied from 0.1 to 1.2%, suggesting that LVD remains quasi-constant over to the range of thresholds considered.

A.2 Lung volume difference analysis

LVD ranged from $8cc$ (0.2%) to more than $1,000cc$ ($>$ 16%) in one case. Table I shows the LVD for each patient and each of the 3 CT scans, in both cc and percentages (gray boxes depict differences greater than 7% noted in patients $n°3$ and $n°4$). Table II depicts LVD repartition in the left and right lungs.

The mean lung density was 0.17 (0.02) g/cm^3 for all images acquired using ABC, and 0.33 (0.15) g/cm^3 for FB scans (standard deviation is given between parentheses), see table III. The increase in lung volume due to the medium DIBH (mDIBH) ranged from 19.5% to 34.5%, depending on the patient ability to perform a deep inspiration and on his FEV1 (Forced Expiratory Volume in the first second).

B. Lung deformation

Table IV, shows for each patient, the mean, median and standard deviation of the displacements of all points in the lung. The table also indicates the mean of the 5% points with the greatest displacement. For each patient, the three CT scans are denoted by A,B,C. Each value in the table is computed according to a mean of the 6 vector fields (AB, BA, AC, CA, BC, CB). Figure 5 represents mean point displacements (in mm) for each patient, in the anterior-posterior (AP), medial-lateral (ML) and cranio-caudal (CC) direction, as well as the 3D norm.

Table V represents mean point displacements in each of the 6 successive vertical lung regions, for left and right

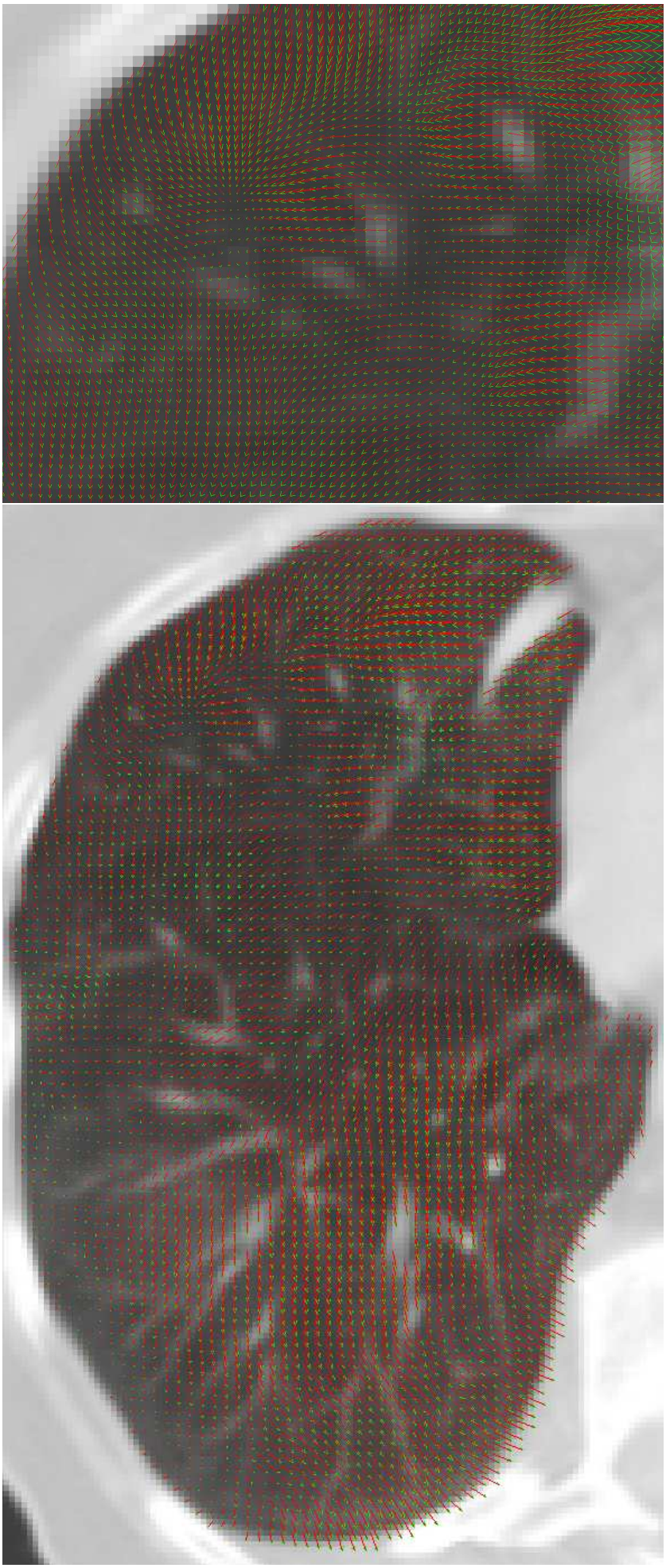

Fig. 2

Example of the orojection of 3D vectors (each sampled at $4\,mm$ for visual purpose). Each point displacement is depicted with a red vector ended by a green arrow.

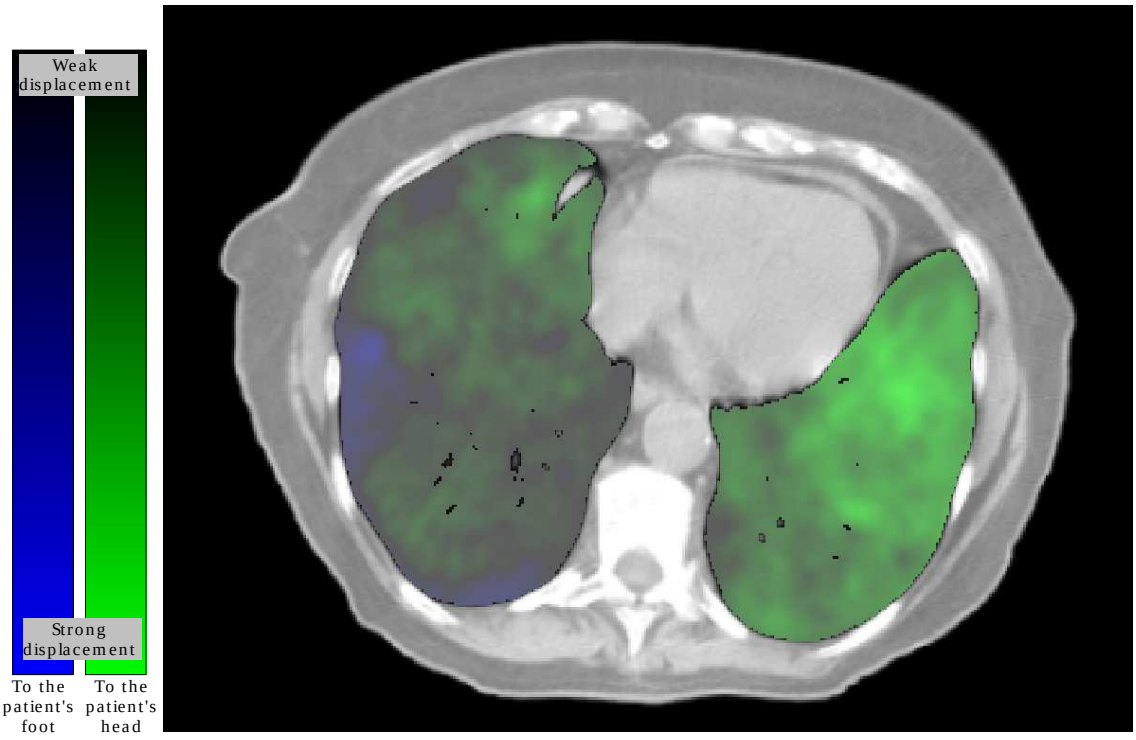

Fig. 3

Cranio-caudal (CC) displacement on an axial slice. Green corresponds to displacements towards patient's head and blue towards patient's foot.

Fig. 4

Norm of 3D vectors on an axial slice. Dark red corresponds to high displacement, light red corresponds to low norm.

Patient	A-B (cc)	B-C (cc)	A-C (cc)	A-B (%)	B-C (%)	A-C (%)
1	148.6	16.5	165.1	3.9%	0.4%	4.1%
2	159.5	80.8	78.7	1.8%	0.9%	0.9%
3	343.2	638.8	309.9	6.6%	13.1%	5.6%
4	603.4	1015.5	412.1	8.9%	16.4%	5.7%
5	134.3	261.4	395.7	1.6%	3.2%	4.8%
6	27.1	72.6	96.6	0.5%	1.3%	1.8%
7	157.9	117.1	40.8	2.8%	2.1%	0.7%
8	47.1	105.7	58.6	0.7%	1.6%	0.9%

TABLE I

LUNG VOLUME DIFFERENCES (LVD) FOR THE THREE CT SCANS (DENOTED BY A,B AND C) OF 8 PATIENTS, EXPRESSED IN *cc* AND IN % OF INITIAL VOLUME. GRAY BOXES POINT TO LARGE VALUES.

Patient	Whole lung		Right lung		Left lung	
	cc	%	*cc*	%	*cc*	%
3	431.2	8.5%	284.2	8.5%	146.5	8.4%
4	698.2	10.6%	196.8	4.2%	506.6	28.1%

TABLE II

LUNG VOLUME DIFFERENCE (LVD) FOR THE LEFT AND RIGHT LUNGS, (IN *cc* AND %) FOR THE THREE PATIENTS SHOWING LARGE LVD.

Patient	FB (g/cm^3)	DI (g/cm^3)	Vol. % change	Density % change
1	0.47	0.20	20.3%	33.9%
2	0.20	0.15	25.4%	5.2%
3	0.51	0.16	18.9%	42.1%
4	0.41	0.17	7.7%	28.5%
5	0.15	0.13	15.4%	1.8%
6	0.23	0.18	34.5%	6.1%
7	0.44	0.18	19.5%	32.4%
8	0.21	0.15	32.7%	6.8%
Mean	0.33	0.17	21.8%	19.6%
Stdev	0.15	0.02	8.8%	16.2%
Mean [8]	0.26	0.19	n.a.	26%
Stdev [8]	0.07	0.04	n.a.	16%

TABLE III

AVERAGE LUNG DENSITIES OF THE 8 PATIENTS MEASURED FROM FB AND DI CT SCANS. THE LAST TWO ROWS DEPICT RESULTS OF HANLEY ET AL. [8] FOR COMPARISON PURPOSE.

Patient	Mean (mm)	Median (mm)	Std dev (mm)	5% max (mm)
1	3.4	2.9	2.0	9.0
2	2.3	1.9	1.4	6.2
3	4.3	3.3	3.3	13.7
4	6.8	5.2	5.1	21.9
5	4.7	4.2	2.5	11.0
6	2.8	2.3	1.8	7.4
7	2.3	1.8	1.7	7.0
8	2.7	2.3	1.5	6.4

TABLE IV

MEAN, MEDIAN, STANDARD DEVIATION OF NORM OF THE DISPLACEMENTS FOR ALL POINTS INSIDE LUNG (FROM $870,000$ TO 2 MILLION POINTS, ACCORDING TO THE PATIENT). FOURTH COLUMN INDICATES THE MEAN OF THE 5% POINTS HAVING GREATEST DISPLACEMENT. EACH COMPUTATION IS AVERAGED OVER 6 VECTOR FIELDS.

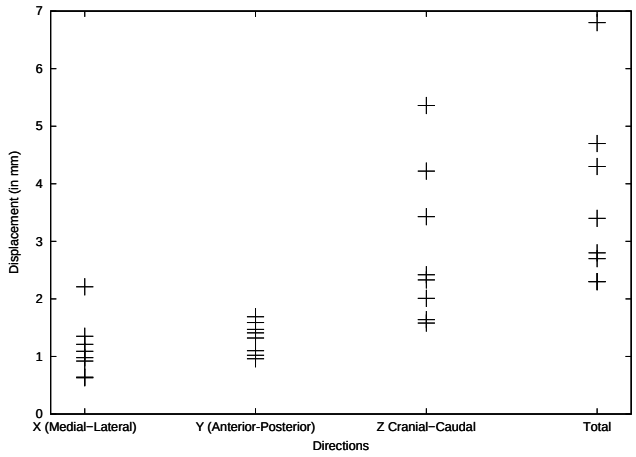

Fig. 5

Mean point displacements (in mm) for each patient, in three directions: X (Medial-Lateral), Y (AnteriorPosterior), Z (Cranio-Caudal) and 3D norm.

lungs (superior 10%, four intermediate 20%, and inferior 10%). For each region, the first 6 rows show mean displacements within the lung volumes, averaged for patients n°$1, 2, 5, 6, 7, 8$ and for patients n°3 and n°4. The next 6 rows show mean displacements on lung surfaces only. The last 6 rows show the mean DTA.

IV. DISCUSSION

A. Compliance / patient tolerance

Among 11 patients with severe respiratory insufficiency, 1 was excluded because he was not able to follow the treatment with ABC, due to inability to understand the procedure. Other patients received 35 fractions with 6 BH daily, leading to a total of more than 200 BH with ABC. The additional time for each session was between 5 and 10 min. This is coherent with other reports such as [20] (approximate extra time, 10 min), or [22] which reports a treatment duration inferior to 20 min. We used a predefined phase of the breathing cycle corresponding to 70% vital capacity (or mDIBH [22]) ; [1] used 80%, [22], [21] used 75%. The BH time was about 20 sec, as in [1], [20], [21], [4] (except that BH time was extended to 30-45 sec for some patients with Hodgkin's cancer in [31] and [1]), or liver cancer in [29].

B. Reproducibility evaluation

Previous studies on BH techniques had shown the necessity of a good reproducibility and the difficulty to evaluate this reproducibility [22], [31], [21], [1]. Indeed, knowing lung displacements allows to determine internal margin (IM), and thus to evaluate the efficiency of the irradiation procedure with BH compares to FB.

2D or 3D techniques can be used to assess this reproducibility. 2D techniques involve the use of radiographic films [29], [20] or portal images [26], [23]. Evaluation is performed by measuring features such as the projection of the top diaphragm cupola relatively to skeleton (assumed to be fixed) [19], [20], [29], [25], or implanted radio-opaque markers [20]. 3D techniques compare several CT scans acquired at equivalent stages. They compare lung volume differences [1], [31], [21], or lung surface distances [1], [22] (using the "A not B; B not A" technique or DTA), or feature points, such as the trachea, the carina, tumor center or the diaphragm, that are (mostly manually) localized on each scan [8], [45], [46].

Results are expressed in terms of CC, AP, ML displacements for 2D studies, and lung volume percentage differences or mean 3D displacements for 3D studies. Reproducibility is generally variable, from $1.0mm$ [23] to $6.6mm$ [20]. Table VI depicts the results of the different studies evaluating BH interfraction reproducibility, with or without ABC.

C. Volume analysis

Patients can be discriminated into two groups (paired t-test shows that the two sets are significantly different) ; the first one (patients $n°1, 2, 5, 6, 7, 8$) has with very good lung volume reproducibility as compared to the second (patients $n°3, 4$).

The first group shows results comparable to previous studies (LVD lower than 4.1% or $170cc$ for the whole lung). Stromberg et al. [31], found 4% mean lung volume differences (at DI) both for intra and inter sessions. Wong et al. [1] found approximately 6% intrafraction (30 min apart) variations of lung volume for three patients. Wilson et al. [21] found inter-fraction LVD varying from 0.2 to 8.7% ($< 186\,cc$) for the right or left lungs (differences are not significant, 10 patients). For comparison, if the lungs were inflated uniformly to a sphere, a LVD of 5% for a $5.7L$ volume would produce to a change in the radius of the sphere of $1.8\,mm$ (maximum displacement); the same calculation for $6.1L$ lung volume with 16% LVD, would lead to $6.3\,mm$ displacement.

Higher differences have been reported in two patients (6 to 16%). Wilson et al. [21] mention one patient with 13.2% ($289cc$) LVD for the left lung (according to the authors, the

Regions	p°1, 2, 5, 6, 7, 8		p°3, 4			
	left	right	left	right		
Volume : mean (stdev) displacement norm						
1 (superior 10%)	2.0(0.7)	1.8(0.7)	2.7(1.0)	2.4(0.8)		
2 (next 20%)	2.7(1.7)	2.1(1.0)	3.9(2.0)	3.1(1.6)		
3 (next 20%)	2.7(1.3)	2.5(1.3)	6.1(3.4)	4.2(2.3)		
4 (next 20%)	3.2(1.6)	3.0(1.6)	7.9(4.1)	4.8(2.8)		
5 (next 20%)	3.9(2.0)	3.7(1.8)	8.1(4.5)	8.2(4.5)		
6 (inferior 10%)	4.1(1.9)	4.0(1.6)	8.5(3.5)	9.4(4.2)		
Surface : mean (stdev) displacement norm						
1 (superior 10%)	2.0(0.8)	1.9(0.8)	2.7(1.2)	2.3(0.9)		
2 (next 20%)	2.6(1.7)	2.2(1.1)	3.8(2.1)	2.9(2.1)		
3 (next 20%)	2.5(1.2)	2.4(1.3)	6.1(3.6)	4.3(3.1)		
4 (next 20%)	2.7(1.5)	2.8(1.6)	7.6(4.2)	4.3(3.2)		
5 (next 20%)	3.4(1.9)	3.5(1.9)	8.0(4.7)	6.1(4.5)		
6 (inferior 10%)	3.9(2.1)	4.1(1.8)	8.2(3.5)	8.2(4.5)		
DTA : Distance To Agreement					[22]	
	left	right	left	right	left	right
1 (superior 10%)	0.7(1.1)	1.0(1.4)	0.8(1.1)	1.1(1.3)	1.6(1.1)	1.4(1.2)
2 (next 20%)	0.7(1.2)	1.0(1.7)	1.0(1.6)	1.6(2.2)	1.1(1.1)	1.2(1.1)
3 (next 20%)	0.6(1.2)	1.0(1.7)	0.7(1.3)	2.1(2.7)	1.0(1.1)	1.0(1.1)
4 (next 20%)	0.7(1.3)	1.1(1.7)	0.7(1.4)	2.5(2.9)	1.1(1.2)	1.3(1.3)
5 (next 20%)	1.2(1.9)	2.3(3.3)	1.0(1.5)	3.4(3.5)	1.9(2.2)	1.7(1.9)
6 (inferior 10%)	3.6(2.9)	4.4(4.0)	1.5(1.8)	4.7(3.3)	2.1(2.1)	2.0(1.8)

TABLE V

LEFT AND RIGHT LUNGS ARE SPLIT INTO SIX CONSECUTIVE REGIONS NORMALIZED TO THE LEFT AND RIGHT LUNG HEIGHT (SUPERIOR 10%, FOUR INTERMEDIATE 20% AND INFERIOR 10%). FOR EACH REGION, THE FIRST 6 ROWS SHOW THE MEAN DISPLACEMENTS INSIDE THE WHOLE LUNG VOLUMES, AVERAGED FOR PATIENTS N°1, 2, 5, 6, 7, 8, AND FOR PATIENTS N°3, 4. THE NEXT 6 ROWS SHOW THE MEAN DISPLACEMENTS ON LUNG SURFACES ONLY. FINALLY, THE LAST 6 ROWS SHOW THE MEAN DTA (DISTANCE TO AGREEMENT) COMPARED TO RESULTS OF [22].

difference seems seemed to be due to restitution of lung volume caused by response of tumor to treatment rather than failure of ABC). Results reported for patient $n°3$ show that the difference is almost equally distributed (8.4%) in each lung, whereas in patient $n°4$ most of the difference is localized in the left lung (28%).

In two patients the discrepancies observed could have clinical causes. Patient $n°3$ had an important emphysema of about $512cc$ in the left lung, and numerous other smaller emphysema foci near the apex. Moreover, he had a pleural effusion that increased between acquisitions and right lower lobe atelectasis. Patient $n°4$ also had atelectasis and decreasing pleural effusion, together with a very low FEV1 (0.7). Both were very tired patients. We conclude that patients with pleural effusion or atelectasis should not be treated with ABC device.

The lung volume increases with BH as compared to FB (average 25%), but remains under levels reported in [4] (average 42%, range $23-66\%$), and comparable to results presented in [8]. This lower increase is probably due to two reasons: all the patients have severe respiratory insufficiency and we have used mDIBH rather than DIBH.

D. Lung deformation

As expected, we first observed a correlation between LVD and mean displacements, with the mean increasing as a function of the. However, two patients (3 and 5) had similar mean displacements ($4.3mm$) but different LVD (4.8% vs 8.4%). The standard deviation of displacement is more linearly related to the LVD (reduced chi-square is 1.0, vs 2.0 for mean).

As in [22], we have observed less displacements in the upper regions of the lung than in the lower parts(table V). However, (1) displacements observed in our study are greater than in [22], and (2) the differences between upper and lower regions are also greater (1.9 to 4, vs 1.5 to 2.1, mean left/right). Our approach has 2 differences. First, we average the distance for each point in the volume and not only on the surface. Second, we compute the distance for the estimated displacement of each point, not its distance to the closest point. This technique allows to avoid a potential problem of DTA which could tend to underestimate motion (for example in the case of vertical sliding). In table V, DTA computation shows lower values than computed displacements. Volume computation also allows to avoid the step of internal extrapolation needed in the surface-based approach.

One important point is the subtraction of the global setup error between the different CT acquisitions. This error is estimated with an automated rigid registration algorithm focusing on the bony parts of the scan. A majority of patients have very low setup errors (lower than 1°,

Dim	Ref	mm (stdev)	Features	A/P	Level	Site	Method
2D	Remouchamps [26] 2003	CC=3.2 ML=2.4 rot=1° CC=3.1 ML=2.3 rot=1°	field border (med. beam) field border (lat. beam)	ABC	mDIBH	breast	EPID (field border), skin tatoo for setup
2D	Balter [29] 2002	AP=2.3 ; ML=2.1 CC=2.5	Skeleton Diaphragm	ABC	NE	liver	CT/Film comparisons Radiographs
2D	Dawson [20] 2001	CC=6.6 ; AP=3.2 ; ML=3.2 CC=4.4	Hepatic microcoils Diaphragm	ABC	NE	liver	Radiographs, microcoils
2D	Kim [25] 2001	CC<5	Diaphragm	Self	NE/NI DE/DI	NSCLC	fluoroscopy, film, video
2D	Mah [23] 2000	from -12 to 11 / 1.3(5.3) range=9.1 0.2 (1.4)	Diaphragm GTV center	Self	DI	NSCLC	Portal films
2D	Hanley [8] 1999	2.5(1.6)	Diaphragm	Self	DI	NSCLC	Fluoroscopy
3D	Cheung [4] 2003	CC=1.1(3.5) AP=1.2(2.3) ML=0.3(1.8)	GTV center	ABC	DI	NSCLC	5 CT
3D	Onishi [44] 2003	CC= 2.2(1.1) AP= 1.4(0.6) ML= 1.3(0.5)	Tumor	Self	DI	NSCLC	3 CT
3D	Remouchamps [22] 2003	1.4(1.7) 1.4(1.0) 1.9 (2.2)	Lung surface Trachea Diaphragm	ABC	mDIBH	breast	2 CT, DTA
3D	Onishi [45] 2003	CC=2.1 AP=1.4 ML=1.3 CC=3.1 AP=2.4 ML=2.2	Tumor Tumor	Self	DI	lung	3 CT(active mode) 3 CT (passive mode)
3D	Wilson [21] 2003	0.2 to 8.7 %, max=13.2%	Lung volume	ABC	mDIBH	NSCLC	3 CT
3D	Qtromberg [31] 2000	4.0%	Lung volume	ABC	DI	Hodgkin	5 CT
3D	Wong [1] 1999	6.0%	Lung volume	ABC	NE / DI	lung liver Hodgkin	2 CT
3D	Hanley [8] 1999	lat width=1.1%; AP height=1.5% lung area = 3%	Overlapping sclices	Self	DI	NSCLC	2-4 CT

TABLE VI

REVIEW OF INTERFRACTION REPRODUCIBILITY STUDIES. CC = CRANIO-CAUDAL ; AP = ANTERIORPOSTERIOR ; ML = MEDIAL-LATERAL ; ABC = ACTIVE BREATH CONTROL ; DIBH = DEEP INSPIRATION BREATH HOLD; MDIBH = MEDIUM DIBH ; NE = NEAR END OF NORMAL EXPIRATION ; NI = NEAR END OF NORMAL INSPIRATION ; DE = DEEP EXPIRATION ; EPID = ELECTRONIC PORTAL IMAGING DEVICE ; DTA = DISTANCE TO AGREEMENT

$2\,mm$), except for some scans acquired at several days interval. In some cases, we detected and correct setup errors up to $30\,mm$.

The drawback of the proposed method are as the follows: precision depends on the slice thickness ($5\,mm$ here) which may overestimate displacements in the CC direction. We used linear interpolation throughout the computation step, which tends to smooth high gradients. Lower slice thickness ($3\,mm$) or high order interpolation methods (such as cubic spline) can improve accuracy. Another drawback is that we do not know whether displacements observed arise from BH differences or from anatomical changes between CT scan (tumor regression for instance). While lung are immobilized, some studies have evaluated the influence of cardiac motion on the treatment of tumors located near the heart. Results presented in [13], [47], [17] have shown that heart beats may not have significant statistical impact on tumor motion. We did not investigate this effect here.

The proposed method also presents valuable advantages. It is automated. It does not require the determination of corresponding points in each CT scan and consequently does not depend on the accuracy of this selection. Besides, it measures 3D information in the whole lung volume: studying the region around the tumor will help calculate internal margins.

V. CONCLUSION

BH techniques are promising but reproducibility evaluation is a prerequesite before allowing to precisely define IM. In this study, we have proposed an original method for evaluating 3D interfraction BH reproducibility. It relies on both rigid and non-rigid registration methods, allowing to compute the "residual error" corresponding to the 3D displacement of each point of a CT scan. We have reported results bases on CT scans of patients enrolled in a phase II trial, for whom 3 CT scan images have been acquired in BH using an ABC device. We have also analyzed lung volume differences and patient compliance.

Active BH with ABC is generally well tolerated, even when patients have severe respiratory insufficiency. For 6 patients, BH was effective and reproducibility was comparable to other interfraction studies. The other two patients have shown insufficient reproducibility, with discrepancies due to clinical reasons.

3D automated computation tools presented here, such as lung volume measurement and deformation field computation, allow for personalized evaluation of breath hold reproducibility. However, drawbacks are the great thickness of the slices, leading to potential inaccuracy in the CC direction, the need to acquire several CT scans, the large amount of data to process.

This study shows the importance of quantifying internal displacements that vary with each patient's respiratory capacity. Because the tools described provide 3D information on each part of the patient's body, the technique can be used to adapt internal margins. It can also be used to quantify patient anatomical evolution during treatment provided that CT scans are acquired regularly (each week, for example). We also plan to use such this information to build a patient-adapted 3D breathing model in order to derive 4D dosimetric studies.

References

[1] JW. Wong, MB. Sharpe, DA. Jaffray, VR. Kini, JM. Robertson, JS. Stromberg, and AA. Martinez. The use of active breathing control (ABC) to reduce margin for breathing motion. *Int J Radiat Oncol Biol Phys*, 44(4):911–19, 1999.

[2] KM. Langen and DT. Jones. Organ motion and its management. *Int J Radiat Oncol Biol Phys*, 50(1):265–78, 2001.

[3] M. Mehta, R. Scrimger, R. Mackie, B. Paliwal, R. Chappell, and J. Fowler. A new approach to dose escalation in non-small-cell lung cancer. *Int J Radiat Oncol Biol Phys*, 49(1):23–33, 2001.

[4] PC. Cheung, KE. Sixel, R. Tirona, and YC. Ung. Reproducibility of lung tumor position and reduction of lung mass within the planning target volume using active breathing control (ABC). *Int J Radiat Oncol Biol Phys*, 57(5):1437–42, 2003.

[5] H.A. Shih, S.B. Jiang, K.M. Aljarrah, K.P. Doppke, and N.C. Choi. Planning target volume determined with fused CT images of fast, breath-hold, and four second simulation ct scans to account for respiratory movement in 3D-CRT in lung cancer. In *ASTRO*, 2002.

[6] K. Tsujino, S. Hirota, M. Endo, K. Obayashi, Y. Kotani, M. Satouchi, T. Kado, and Y. Takada. Predictive value of dose-volume histogram parameters for predicting radiation pneumonitis after concurrent chemoradiation for lung cancer. *Int J Radiat Oncol Biol Phys*, 55(1):110–5, 2003.

[7] Y. Seppenwoolde, K. De Jaeger, and JV. Lebesque. In regard to tsujino et al.: predictive value of dose-volume histogram parameters for predicting radiation pneumonitis after concurrent chemoradiation for lung cancer. *Int J Radiat Oncol Biol Phys*, 56(4):1208–9, 2003.

[8] J. Hanley, MM. Debois, D. Mah, GS. Mageras, A. Raben, K. Rosenzweig, B. Mychalczak, LH. Schwartz, PJ. Gloeggler, W. Lutz, CC. Ling, SA. Leibel, Z. Fuks, and GJ. Kutcher. Deep inspiration breath-hold technique for lung tumors: the potential value of target immobilization and reduced lung density in dose escalation. *Int J Radiat Oncol Biol Phys*, 45(3):603–11, 1999.

[9] K. Yamada, T. Soejima, E. Yoden, T. Maruta, T. Okayama, and K. Sugimura. Improvement of three-dimensional treatment planning models of small lung targets using high-speed multislice computed tomographic imaging. *Int J Radiat Oncol Biol Phys*, 54(4):1210–6, 2002.

[10] T. Neicu, H. Shirato, Y. Seppenwoolde, and SB. Jiang. Synchronized moving aperture radiation therapy (smart): average tumour trajectory for lung patients. *Physics in Medecine and Biology*, 48(5):587–598, 2003.

[11] L. Ekberg, O. Holmberg, L. Wittgren, G. Bjelkengren, and T. Landberg. What margins should be added to the clinical target volume in radiotherapy treatment planning for lung cancer? *Int J Radiat Oncol Biol Phys*, 48(1):71–7, 1998.

[12] C. Ozhasoglu and MJ. Murphy. Issues in respiratory motion compensation during external-beam radiotherapy. *Int J Radiat Oncol Biol Phys*, 52(5):1389–99, 2002.

[13] Y. Seppenwoolde, H. Shirato, K. Kitamura, S. Shimizu, M. van Herk, and JV. Lebesque. Precise and real-time measurement of 3D tumor motion in lung due to breathing and heartbeat, measured during radiotherapy. *Int J Radiat Oncol Biol Phys*, 53(4):822–34, 2002.

[14] S. Essapen, C. Knowles, and D. Tait. Variation in size and position of the planning target volume in the transverse plane owing to respiratory movement during radiotherapy to the lung. *Br J Radiol.*, 74(877):73–6, 2001.

[15] CW. Stevens, RF. Munden, KM. Forster, JF. Kelly, Z. Liao, G. Starkschall, S. Tucker, and R. Komaki. Respiratory-driven lung tumor motion is independent of tumor size, tumor location, and pulmonary function. *Int J Radiat Oncol Biol Phys*, 51(1):62–8, 2001.

[16] P. Giraud, Y. De Rycke, B. Dubray, and et al. Conformal radiotherapy planning for lung cancer: analysis of intrathoracic organ motion during extreme phases of breathing. *Int J Radiat Oncol Biol Phys*, 51(4):1081–1092, 2001.

[17] S. Shimizu, H. Shirato, K. Kagei, and et al. Impact of respiratory movement on the computed tomographic images of small lung tumors in three-dimensional (3D) radiotherapy. *Int J Radiat Oncol Biol Phys*, 46(5):1127–1133, 2000.

[18] EC. Ford, GS. Mageras, E. Yorke, R. Rosenzweig KE, Wagman, and CC. Ling. Evaluation of respiratory movement during gated radiotherapy using film and electronic portal imaging. *Int J Radiat Oncol Biol Phys*, 52(2):522–31, 2002.

[19] R. Wagman, E. Yorke, E. Ford, P. Giraud, G. Mageras, B. Minsky, and K. Rosenzweig. Respiratory gating for liver tumors: use in dose escalation. *Int J Radiat Oncol Biol Phys*, 55(3):659–68, 2003.

[20] LA. Dawson, KK. Brock, S. Kazanjian, D. Fitch, CJ. McGinn, TS. Lawrence, RK. Ten Haken, and J. Balter. The reproducibility of organ position using active breathing control (ABC) during liver radiotherapy. *Int J Radiat Oncol Biol Phys*, 54(1):1410–21, 2001.

[21] EM. Wilson, FJ. Williams, BE. Lyn, JW. Wong, and EG. Aird. Validation of active breathing control in patients with non-small-cell lung cancer to be treated with CHARTWEL. *Int J Radiat Oncol Biol Phys*, 57(3):864–74, 2003.

[22] VM. Remouchamps, N. Letts, D. Yan, FA. Vicini, M. Moreau, JA. Zielinski, J. Liang, LL. Kestin, AA. Martinez, and JW. Wong. Three-dimensional evaluation of intra- and interfraction immobilization of lung and chest wall using active breathing control: a reproducibility study with breast cancer patients. *Int J Radiat Oncol Biol Phys*, 57(4):968–78, 2003.

[23] D. Mah, J. Hanley, KE. Rosenzweig, E. Yorke, CC. Braban L, Ling, SA. Leibel, and G. Mageras. Technical aspects of the deep inspiration breath-hold technique in the treatment of thoracic cancer. *Int J Radiat Oncol Biol Phys*, 48(4):1175–85, 2000.

[24] W.G. O'Dell, M.C. Schell, D. Reynolds, and P. Okunieff. Dose broadening due to target position variability during fractionated breath-held radiation therapy. *Med Phys*, 29(7):1430–1437, 2002.

[25] DJ. Kim, BR. Murray, R. Halperin, and WH. Roa. Held-breath self-gating technique for radiotherapy of non-small-cell lung cancer: A feasibility study. *Int J Radiat Oncol Biol Phys*, 49(1):43–49, 2001.

[26] VM. Remouchamps, N. Letts, FA. Vicini, MB. Sharpe, LL. Kestin, PY. Chen, AA. Martinez, and JW. Wong. Initial clinical experience with moderate deep-inspiration breath hold using an active breathing control device in the treatment of patients with left-sided breast cancer using external beam radiation therapy. *Int J Radiat Oncol Biol Phys*, 56(3):704–15, 2003.

[27] VM. Remouchamps, FA. Vicini, MB. Sharpe, LL. Kestin, AA. Martinez, and JW. Wong. Significant reductions in heart and lung doses using deep inspiration breath hold with active breathing control and intensity-modulated radiation therapy for patients treated with locoregional breast irradiation. *Int J Radiat Oncol Biol Phys*, 55(2):392–406, 2003.

[28] KL. Baglan, MB. Sharpe, D. Jaffray, RC. Frazier, J. Fayad, LL. Kestin, V. Remouchamps, AA. Martinez, J. Wong, and FA. Vicini. Accelerated partial breast irradiation using 3D conformal radiation therapy (3D-CRT). *Int J Radiat Oncol Biol Phys*, 55(2):302–11, 2003.

[29] JM. Balter, KK. Brock, DW. Litzenberg, DL. McShan, TS. Lawrence, R. Ten Haken, CJ. McGinn, KL. Lam, and LA. Dawson. Daily targeting of intrahepatic tumors for radiotherapy. *Int J Radiat Oncol Biol Phys*, 52(1):266–71, 2002.

[30] KE. Sixel, MC. Aznar, and YC. Ung. Deep inspiration breath hold to reduce irradiated heart volume in breast cancer patients. *Int J Radiat Oncol Biol Phys*, 49(1):199–204, 2001.

[31] JS. Stromberg, MB. Sharpe, LH. Kim, VR. Kini, DA. Jaffray, AA. Martinez, and JW. Wong. Active breathing control (ABC) for hodgkin's disease: reduction in normal tissue irradiation with deep inspiration and implications for treatment. *Int J Radiat Oncol Biol Phys*, 48(3):797–806, 2000.

[32] S. Hu, E.A. Hoffman, and J.M. Reinhardt. Automatic lung segmentation for accurate quantitation of volumetric X-ray CT images. *IEEE T Med Im*, 20(6):490–8, 2001.

[33] B. Zitova and J. Flusser. Image registration methods: a survey. *Im. Vis. Comp.*, 21:977–1000, 2003.

[34] F.L. Bookstein. Principal warps: Thin-plate splines and the decomposition of deformations. *IEEE T Pat An Mach Int*, 11:567–585, 1989.

[35] J.P. Thirion. Image matching as a diffusion process: an analogy with Maxwell's demons. *Medical Image Analysis*, 2(3):243–260, 1998.

[36] P. Cachier and N. Ayache. Regularization in image non-rigid registration: I. trade-off between smoothness and intensity similarity. Technical Report 4188, inria, 2001.

[37] P. Cachier and N. Ayache. Regularization methods in non-rigid registration :ii. isotropic energies, filters and splines. Technical Report 4243, inria, 2001.

[38] S. Clippe V. Boldea, D. Sarrut. Lung deformation estimation with non-rigid registration for radiotherapy treatment. In *MICCAI'2003*, volume 2878, pages 770–7. LNCS, 2003.

[39] B.K.P. Horn and B. Schunk. Determining optical flow. *Artificial Intelligence*, 17:185–203, 1981.

[40] R. Deriche. Recursively implementing the gaussian and its derivatives. Technical Report 1893, INRIA, apr 1993.

[41] M. Bro-Nielsen and C. Gramkow. Fast fluid registration of medical images. In K.H. Hone and R. Kikinis, editors, *vbc*, volume 1131, pages 267–276. lncs, 1996.

[42] F. Maes, A. Collignon, D. Vandermeulen, G. Marchal, and P. Suetens. Multimodality Image Registration by Maximization of Mutual Information. *IEEE T Med Im*, 16(2):187–198, 1997.

[43] W.M. Wells, P.A. Viola, H. Atsumi, S. Nakajima, and R. Kikinis. Multi-Modal Volume Registration by Maximization of Mutual Information. *Medical Image Analysis*, 1(1):35–51, 1996.

[44] P.E. Danielsson. Euclidean distance mapping. *Computer Graphics and Image Processing*, 14:227–248, 1980.

[45] H. Onishi, K. Kuriyama, T. Komiyama, S. Tanaka, N. Sano, and Y. Aikawa. A new irradiation system for lung cancer combining linear accelerator, computed tomography, patient self-breath-holding, and patient-directed beam-control without respiratory monitoring devices. *Int J Radiat Oncol Biol Phys*, 56(1):14–20, 2003.

[46] H. Onishi, K. Kuriyama, T. Komiyama, S. Tanaka, J. Ueki, N. Sano, T. Araki, S. Ikenaga, Y. Tateda, and Y. Aikawa. Ct evaluation of patient deep inspiration self-breath-holding: how precisely can patients reproduce the tumor position in the absence of respiratory monitoring devices? *Med Phys*, 30(6):1183–7, 2003.

[47] H. Shirato, S. Shimizu, K. Kitamura, T. Nishioka, K. Kagei, S. Hashimoto, H. Aoyama, T. Kunieda, N. Shinohara, H. Dosaka-Akita, and K. Miyasaka. Four-dimensional treatment planning and fluoroscopic real-time tumor tracking radiotherapy for moving tumor. *Int J Radiat Oncol Biol Phys*, 48(2):435–42, 2000.